Endogenous social distancing and its underappreciated impact on the epidemic curve

Sebastian Funk[a], **Marko Gosak**[b,c], **Moritz U. G. Kraemer**[d,e], **Heinrich H. Nax**[f,g,*], **Matjaž Perc**[b,h,i], **and Bary S. R. Pradelski**[j]

[a]London School of Hygiene and Tropical Medicine, Keppel St, WC1E 7HT London, UK; [b]Faculty of Natural Sciences and Mathematics, University of Maribor, Koroška cesta 160, 2000 Maribor, Slovenia; [c]Faculty od Medicine, University of Maribor, Taborska ulica 8, 2000 Maribor, Slovenia; [d]Department of Zoology, Mansfield Road, University of Oxford, OX1 3SZ Oxford, UK; [e]Harvard Medical School, 25 Shattuck St, 02115 Boston, USA; [f]Behavioral Game Theory, Clausiusstrasse 37, ETH Zurich, 8092 Zurich, CH; [g]Institute of Sociology, Andreasstrasse 15, University of Zurich, 8050 Zurich, CH; [h]Department of Medical Research, China Medical University Hospital, China Medical University, Taichung, Taiwan; [i]Complexity Science Hub Vienna, Josefstädterstraße 39, A-1080 Vienna, Austria; [j]Univ. Grenoble Alpes, CNRS, Inria, Grenoble INP, LIG, 38000 Grenoble, France

This manuscript was compiled on May 9, 2020

Social distancing is an effective strategy to mitigate the impact of infectious diseases. If either sick or healthy individuals, or both, socially distance, the epidemic curve flattens. Substantial amounts of contact reductions occur endogenously during a disease outbreak: Some are due to health-related mobility loss (severity of symptoms), duty of care for an infected person in the same household, and forced quarantine. Other changes are due to voluntary social distancing. In particular, sick people reduce contacts to avoid infecting others, and healthy individuals do so in order to stay healthy. We use game theory to formalize the interaction involving voluntary social distancing in a partially infected population. This improves the behavioral micro-foundations of epidemiological models and predicts differential social distancing dependent on health status. The model's key predictions in terms of comparative statics are derived, which concern changes and interactions of endogenous differential social distancing behaviors. We fit the relevant parameters for endogenous social distancing in an epidemiological model with evidence from influenza waves and the current COVID-19 pandemic, and use these fits to provide a benchmark for an epidemic curve with endogenous social distancing. Our results suggest that a curve similar in peak and case numbers to what resulted from a lockdown, yet quicker to pass, could have occurred endogenously. Going forward, eventual social distancing orders and policies should be benchmarked against more realistic curves that take endogenous social distancing into account, rather than be driven by unrealistic horror scenarios that are based on static estimates for social mixing.

Social distancing | Game theory | Disease spreading | Contact rates

The contact rates of infectious and non-infectious agents play a key role in determining the epidemic curve. For example, when individuals infected with the SARS-CoV-2 virus have limited contact with susceptible individuals because of rapid case-isolation policies, transmission can be reduced effectively (1). How effective less stringently enforced policies and recommendations of social distancing or isolation are depends in general on the individual-level decisions regarding whether or not to adhere to social distancing voluntarily and/or in response to social distancing policies.

Governments seem to disagree strongly regarding how much freedom of choice their citizens are ideally entrusted with in order to achieve social distancing, resulting in less (e.g. Sweden) and more (e.g. China) stringent policies. To identify adequate policy responses, it is important to understand *behavioral change* in epidemiological models (see reviews by (2–4)). However, the interactive nature of the behavioural change in social distancing during infectious disease outbreaks (in contrast to the contexts of decisions for vaccination (5–7) and antiviral prophylaxis (8)) have not been explored in much detail, in particular not regarding the individual-level game-theoretic foundations of social distancing, and how these compare with real-world evidence. Progress in this direction ought to be made, because game-theoretic analyses have shown that interactions can crucially shape the epidemic curve (9–11), and modeling increasingly rests on rich assumptions regarding how individual behavior changes dynamically with the disease outbreak.

In the context of policy-relevant COVID-19 modelling, some assumptions made regarding behavioral change had to be made without adequate empirical foundations. The early simulations "driving the world's response to COVID-19" (12), for example, were based on static estimates of social mixing. These simulations painted horrific scenarios in terms peak and case numbers of the outbreak, which led to the introduction of social distancing policies across (most of) the globe. To evaluate which policies should be used, modelers again made assumptions regarding how social distancing policies would be adopted in terms of reductions of the population—as this example on how a population would respond to a recommendation of voluntary home quarantine from (13) illustrates: "Following identification of a symptomatic case in the household, all household members remain at home for 14 days. Household contact rates double during this quarantine

period, contacts in the community reduce by 75%. Assume 50% of household comply with the policy.".

What numbers are chosen precisely is important to justify policies, yet it is unclear what these particular ones were based on—theory, evidence or introspection. What is clear is that understanding the exact nature of individual-level incentives and responses underlying decision-making better is important as it helps to elucidate when and whether there are conflicts of interest between individual and collective interests (5), or not (14). This is an important factor when governments choose between health and mobility recommendations and forced quarantine and lockdown measures. Hence modeling must move from making mobility assumptions to theoretically and empirically validated mobility ingredients. Here, making such a step toward establishing a suitable framework for integrating behavioral micro-foundations of mobility, we draw on game theory to embed interactive decision-making of social distancing in an epidemiological model.

Recently, many countries enforced strict restrictions on movements and social interactions, because the general impression was that voluntary social distancing recommendations would not be sufficient (15). Quite plausibly, due to the large economic and social impact of country-wide lockdowns, governments increasingly consider restricting human movements and social contact dependent on health and risk status so as not to lock down the entire population (16). The issue is that research has not yet provided empirical benchmarks for differential mobility in disease scenarios, so it is unclear how such policies can be evaluated: Any policies aimed at reducing mobility should be benchmarked against what mobility would have been without such policies in light of the disease, not against what mobility was like before the disease. We here propose a game-theoretic model of social distancing behavior in order to provide avenues for formulating such benchmarks, and compare its predictions to observations of contact rates during two influenza seasons in the United Kingdom where human contact was not affected by specific government restrictions. The observed restrictions might be viewed as lower bounds on the counterfactual endogenous levels of social distancing that ought to be expected in the current COVID-19 situation if no explicit policies had been imposed. We show that levels of endogenous social distancing as would be expected from an influenza season would already flatten the epidemic curve substantially, and that social distancing orders would really have to be quite effective to warrant their introduction given such counterfactuals.

Modelling infectious disease dynamics

The close monitoring and detailed modeling of outbreaks of infectious diseases has become an increasingly active research focus in epidemiology since the seminal works by (17–19) and (20, 21). Over the past decades, the emergent body of epidemiological research has substantially improved our understanding of the dynamics of infectious diseases as well as how to control and prevent them (e.g. vaccination, quarantine, social distancing policies, etc. (22–24)), which together with the increasing availability of relevant data has

Significance Statement

Infectious disease transmission in human populations crucially depends on contact patterns during outbreaks: *Who makes which contacts when?* An underappreciated element of contact behaviors is their interactive nature, and the cost-benefit analyses driving them. Endogenizing interactive cost-benefit analyses that factor in both infection risk and health status crucially changes predictions for the epidemic curve in ways that state-of-the-art epidemiological modeling does not capture. We look at data and find empirical evidence for health status dependent social distancing, as well as for other behaviors predicted by our theory. We run empirically informed simulations based on our model, and show that levels of curve flattening ought to be expected that match rather draconic lockdown policies, but they are endogenous and not imposed.

All authors contributed to all aspects of the paper, with M.U.G.K. and H.H.N. designing the study, and B.S.R.P. and H.H.N. modeling, M.G. and M.P. simulating, and S.F. working with Flusurvey.

There are no conflicting interests to declare.

[2]To whom correspondence should be addressed. E-mail: heinrich.nax@uzh.ch

allowed to apply some of these models to real-world epidemics.

One key modeling aspect concerns the transmission of infectious pathogens via individual contacts between infectious and susceptible individuals (25, 26), which have been shown to differ dependent on demographic factors such as age and sex (27–29). While a lot of previous work focuses on reconstructing the transmission trees of observed epidemics (30), or on their final size and geographic spread (31, 32), less attention has been paid to the role that individual decision-making regarding social distancing –weighing the risks of infecting and being infected– plays in shaping behavioral contact patterns that underlie these dynamics.

Mobility or, more generally, contact-seeking/avoiding decisions are key drivers of disease dynamics. Descriptive analyses of individual human mobility have revealed remarkable consistency at multiple temporal and spatial scales in the absence of exogenous factors (33–37), but also revealed that contact patterns change as a result of disease severity (38). One roadblock for making progress has been that contact and movement data are typically collected independently of health status.* While this is currently changing with emerging health-tracking applications, there is no robust data that has been made available as of now. As a consequence, there is little empirical evidence on how human contact rates change depending on health status and as a function of disease incidence overall –often due to the lack of available real-time contact information (40).† Precisely this kind of insight, however, would be important to advance the understanding of the interactive nature of contact rate decisions, because the incentives to practice social distancing or not are different for healthy and for sick people. To improve predictions concerning the dynamics of diseases at the population level (43), and to understand what kinds of policies are actually appropriate, uncovering the behavioral determinants of contact patterns is therefore an important next step as applied work until now has to work largely by making crude assumptions, which may be sensitive, especially during the key (early) periods of an epidemic.

A rational-choice foundation of individual contact-seeking/avoiding behaviour in response to an infectious disease in epidemiological models is a framework proposed by (44). The result is a model where the contact rates of the resulting epidemiological model are no longer exogenous variables, but instead are determined co-evolutionarily with the dynamics of the disease itself. (44)'s framework presents an individual risk assessment, presuming that individuals' propensities to stay home (more social distancing) increase with intensity and awareness of the disease due to the increased risks for contracting the disease. The simulations presented in (44) show that incorporating this type of individual decision-making changes predictions concerning the epidemic curve: (much) flatter curves are the result, particularly if sick individuals also reduce their contacts.

The decision-theoretic framework by (44) is a primer toward integrating human behavior into disease modeling, especially as regards understanding the role of infection fear in shaping contact patterns. To improve the behavioral micro-foundations of disease modeling, the aim of which is to better predict epidemic dynamics and to deliver more effective intervention policies, we generalize the existing decision-theoretic framework in two ways. First, the contact-reduction results are checked against some data on contact patterns during the 2012 and 2013 flu epidemics in the United Kingdom. Second, going beyond the single-player decision-theoretic approach, which does not account for the interactive nature of contact decisions, the underlying theoretical framework is extended to a game-theoretic model. By using game theory we can model not just the trajectory of the disease as a function of the underlying contact data, but more generally endogenize contact patterns by an interactive decision model and as determined by the dynamics of the disease (e.g., incidence rates). The framework proposed improves the rational-choice foundations of epidemiological models towards an integrated co-evolutionary view on contact rates and disease dynamics, which may substantially advance its predictive potential.

The core argument of this paper is that the kinds of risk assessments underlying contact decisions are interactive, which we model using game theory by formulating what we shall call "the social distancing

*See (39) for one of the first studies to do so via a telephone survey conducted during an influenza season.

†Some related empirical work has been done to capture the change in human movements in response to environmental disaster (41), and travel restrictions (42), but not in response to disease outbreaks except for some recent work we shall discuss separately in the concluding remarks.

game". The model permits us to produce testable individual-level comparative statics regarding how individuals will react during the outbreak of a disease and in response to others' contact patterns (checking against data from two influenza seasons in the UK for some empirics). Looking forward, the advantage of our game-theoretic modeling approach is that it becomes feasible to identify tipping points in the underlying dynamics,[‡] whose transitions may be explosive and differ fundamentally for marginally different starting conditions as compared to those predicted by a non-game-theoretic model (47). The next level of epidemic modeling should therefore consider game-theoretic modelling so as to leverage possible dynamics of equilibrium transitions to policy advantage, as is argued in policy making related to social dynamics (48, 49).

Indeed, there have been two very recent concurrent papers making progress in this direction, and future work could merge our lines of analyses with theirs. The first is by (50) who considers a theoretical model with endogenous contact rates where the two types of agents, sick (and infectious but not yet symptomatic) and healthy, who choose contact rates are in the same information set. Infected individuals stay at home with probability one. Their model generates the same contact rates for both types, and does not make predictions regarding interaction effects of the two. Our data indicates that health status leads to different contact patterns, and that symptomatic individuals also vary contact rates as a function of incidence. This is also an important feature of our simulations. A very nice feature of their model is an explicit treatment of the path dependency of equilibrium, which would be nice to extend to a framework like ours too in future work. The second paper is a related theoretical framework by (51) who do not consider endogenous contact reductions by infected individuals at all because they have no private benefit from it. In that sense their model is more similar to (44) than ours, but adds a Nash equilibrium analysis to it. Again, our data indicates that infected and infectious individuals do also reduce contact rates with incidence levels, and that there are interactions between contact rates of sick and healthy individuals. Pro-social concerns for the health of others, not just concerns for one's own health, clearly play a very important role.

In sum, the ambition of this paper is to integrate behavioral responses from a game-theoretic framework into classical epidemiological models that accounts for health status and includes self-protective and pro-social concerns. By doing so, we propose a new model, spell out its behavioral predictions, in particular regarding differential rates of social distancing. We compare theoretical results with empirical observations from the 2012 and 2013 influenza epidemic in the United Kingdom, and discuss implications for policy recommendations in light of the simulated epidemic curves our model generates. We compare the endogenous curve with curves that would result from interventions such as immobilizing fractions of the population.

Methods

Contact rates. The key ingredients, implicitly behavioral ones, that determine the dynamics of epidemiological models are so-called 'contact rates' which govern the frequency and likelihood of human interactions and therefore transmissions: *Where do you go? Who do you see? How do you make contact?* At the individual level, a change in contact rates may occur for symptom-specific medical reasons after contracting a disease that leads to reduced mobility for example. Moreover, a person, whether infected or not, may consciously decide to social distance, that is, to reduce contacts in light of various evolving risks (i.e. of spreading the disease and/or of contracting the disease) during an outbreak.[§]

To understand the implications of these endogenous phenomena, we need a model for how and why behavioral change occurs during outbreaks of infectious diseases. To do so, we extend the existing decision-theoretic model of (44) to allow for interactive decisions and *strategic* considerations as the risks of contracting and transmitting a disease depend on one's own contact patterns as well as on everyone else's levels of social distancing. Therefore, we model the individual decision as dependent on others' decisions, and we identify the rational-choice predictions for these decisions. By combining the human perspective on decision-making including considerations of risks and interactions in this way –using game theory– we

[‡] See, for example, (45, 46).

[§] We referred to social distancing as self-quarantine in earlier versions of the paper, but adopt this jargon in line with (44) as is becoming standard.

obtain new and testable predictions for how human contact patterns and mobility decisions interact.

To illustrate the interactive nature of the proposed problem, consider the following thought experiments at the two extremes of the logical spectrum. At one extreme, suppose that everyone (sick and healthy alike) stays home, i.e. has reduced their contacts to zero (extreme social distancing). In that case, of course, any given individual (think of Will Smith in "I Am Legend" to lighten the mood) can move freely without fear of infection (if healthy) or of infecting others (if sick). Thus, in game-theoretic language, this does not constitute a Nash equilibrium, because every individual prefers to deviate (from staying at home), given the decision of everyone else (to stay at home). At the other extreme, by contrast, when everyone (sick and healthy) is moving around all the time resulting in very high contact rates (no social distancing), it is safest to stay home in order to not become infected (if healthy) or not to infect others (if sick). Again, everyone moving freely around will not constitute an equilibrium.

Social distancing in a population. In this section, we propose a formal model that will highlight the main advantages of choosing a game-theoretic rather than mechanistic approaches (as is done in applied work), and spell out how it goes beyond a single-player decision-theoretic model.

Population. Consider a human population $N = \{1, 2, ..., n\}$. Each person $i \in N$ either belongs to the set $H \subset N$, the *healthy* (or non-symptomatic, susceptible, uninfected, etc.), or to the other set $S = N \setminus H$, the *sick* (or symptomatic, non-susceptible, infected, etc.).[¶]

Social-distancing decisions. Each $i \in N$ chooses a contact rate $\beta_i \in [0, 1]$. Write β for the full vector of contact rates, β_H for the average contact rate of healthy agents, and β_S for the average contact rate of sick agents.

Utilities. Individual utility is generated by reaching places (or people) which is facilitated by being mobile. Hence, positive mobility is required to generate utility. But increased levels of mobility are also increasingly costly as they increase the exposure to infection risks for self and others. Hence, both complete immobility and full mobility generate no utility. Once there are risks of infection due to the presence of a disease, this mobility will be reduced to mitigate these risks.

Let us consider two scenarios distinguished by whether *i.*) everyone is healthy, or *ii.*) there are infected individuals.

i.) *No-disease scenario.* Suppose there is no disease, that is, $|S| = 0$. In that case, we assume utility for any player i is described by a twice-differentiable, continuous utility function

$$\textbf{Base utility.} \quad u_i(\beta) = u(\beta_i) \tag{1}$$

such that $u(0) = u(1) = 0$, $u(\beta) > 0$ for all $\beta \in (0, 1)$, $u'(\beta) > 0$ (< 0) for $\beta < \beta^*$ ($> \beta^*$) given some $\beta^* \in (0, 1)$, and $u''(\beta) < 0$. These assumptions ensure that β^* represents the unique utility-maximizing level of mobility in the no-disease scenario. We shall refer to levels chosen below β^* as 'social distancing'. Of course, the optimal level will be heterogeneous within a population, but we abstract from this level of detail for the moment.[‖]

ii.) *Disease scenario.* Once some individuals are infected, that is, if $|S| > 0$, then the 'base utility' $u(\beta_i)$ that corresponds to a healthy individual, for an infected individual, is reduced directly by some disease factor δ (with $\delta \in [0, 1]$ representing a proportional disutility from being sick) resulting in 'sick utility' $\delta u(\beta_i)$. Moreover, depending on health status, all individuals suffer additional disutility from the risk of becoming infected (for healthy), or from the risk of infecting others (for sick), both of which increase with mobility, thus adding further costs to being mobile. Hence, for a **healthy individual**, $i \in H$ the utility is

$$\textbf{Healthy } H\textbf{-utility.} \quad u_i(\beta) = \tag{2}$$
$$(1 - f \cdot \underbrace{(1 - [(1 - \beta_S^i)^{n-|H|} \cdot \beta_i + 1 - \beta_i])}_{\text{infection risk}}) \quad \cdot \quad \underbrace{u(\beta_i)}_{\text{base utility}}$$

[¶] Here, we work with a basic epidemic model setting without recovery in mind, which naturally ought to be generalized in future work.

[‖] Recent empirical work by (36, 49) identifies heterogeneous levels of mobility in the absence of a disease.

where $f \in [0,1]$ measures the fear of a healthy individual of getting infected, which would also express how severe the disease is. Similarly, for a **sick individual**, $i \in S$, the utility is

$$\textbf{Sick } S\textbf{-utility.} \quad u_i(\beta) = \underbrace{(1 - c \cdot (1 - [(1-\beta_H^i)^{|H|} \cdot \beta_i + 1 - \beta_i]))}_{\text{spreading risk}} \cdot \underbrace{\delta u(\beta_i)}_{\text{sick utility}} \tag{3}$$

where $c \in [0,1]$ measures the pro-social concern an infected individual has for another individual's life, that is, the expected reduction in utility from exposing other healthy humans to the risk of infection, which would naturally increase with the severity of the disease too. Note that the introduction of this parameter expressing this type of motivation, which is central to most policies aimed at reducing mobility of symptomatic humans, is absent in (44), but will generate the kinds of mobility reductions that characterize several of his simulations resulting in the flattest epidemic curves.

The underlying contact scenario we thus express is one where β_i represents agent i's probability of exposing him/herself to an infection-risk encounter, and 1-(1-β_S^i)$^{n-|H|}$ and 1-(1-β_H^i)$^{|H|}$ respectively represent the probabilities of at least one infected / susceptible making the same encounter. Thus we model the probability of two parties meeting at a given location, or all parties spending some time at a central locations. W.l.o.g., when two individuals with different health status enter the location, we assume an infection takes place with probability one.

Results. What interests us are the comparative statics of rational-choice contact rates in equilibrium when mobility rates are chosen optimally so as to maximize subjective expected utilities. These we identify by inspection of the conditions for optimal behavior for the two utility functions given by Equations 3 and 2, which we obtain by maximizing both expressions with respect to β_i, yielding the two first-order conditions (FOCs):

$$H\textbf{-FOC.} \quad \overbrace{(1 - f \cdot (1 - [(1-\beta_S^i)^{n-|H|} \cdot \beta_i + 1 - \beta_i]))u'(\beta_i)}^{\text{marginal utility effect}} = \underbrace{f \cdot (1 - (1-\beta_S^i)^{n-|H|})u(\beta_i)}_{\text{marginal infection risk effect}} \tag{4}$$

$$S\textbf{-FOC.} \quad \overbrace{(1 - c \cdot (1 - [(1-\beta_H^i)^{|H|} \cdot \beta_i + 1 - \beta_i]))u'(\beta_i)}^{\text{marginal utility effect}} = \underbrace{c \cdot (1 - (1-\beta_H^i)^{|H|})u(\beta_i)}_{\text{marginal spreading risk effect}} \tag{5}$$

Note that both right-hand sides of the latter equations are positive, indicating that both marginal utilities $u'(\beta_i)$s must also be positive; i.e. that we now must obtain lower contact rates for both sick and healthy individuals (compared with the utility-maximizing level of mobility β^* from the no-disease scenario) in order for FOCs to be satisfied than in the no-disease benchmark. This means that both sick and health individuals will engage in some optimal level of 'social distancing', that is, choosing a lower equilibrium utility than β^* from the no-disease scenario.

Comparative statics. From inspection of above two FOCs, we obtain the comparative statics summarized in Table 1.**

Naturally, the optimal contact rates for healthy and sick are different and take intermediate values, the exact value depending on factors related to disease incidence, fear, concern, disease severity, risks, etc. Note

** Comparative statics describe how the optimal contact rate varies with the various other parameters. Here, these are evaluated under the assumption that a symmetric Nash equilibrium exists such that, in equilibrium, $\beta_i = \beta_H$ for all healthy and $\beta_i = \beta_S$ for all sick.

Table 1. Comparative statics of the equilibrium analysis.

A marginal increase in ...	... leads to ...
social distancing of Healthy	less social distancing of Sick.
social distancing of Sick	less social distancing of Healthy.
size of the Healthy population	more social distancing of Sick.[!]
size of the Sick population	more social distancing of Healthy.[!]
pro-social concern of the Sick	more social distancing of Sick.
fear of disease of the Healthy	more social distancing of Healthy.[*]

*: Present in the model by (44). The other effects are new.
!: Contrary to imitation, herding, etc. as proposed, for example, in (10, 52).

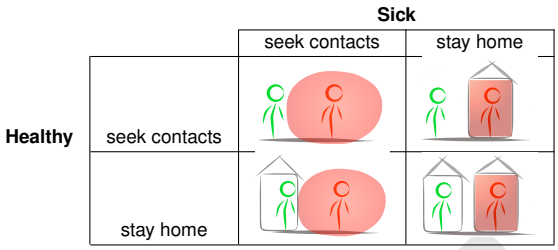

Fig. 1. The social distancing interactions simplified.

that individuals may also differ in their fears, concerns, etc., hence we can think of the comparative statics in Table 1 also as organizing individual heterogeneity. While this is a two-population evolutionary game with continuous action space for every player, the strategic essence of this interaction can be represented by a simplified game played between Sick and Healthy as is illustrated in **Fig.** 1. Both health types seek contact leads to infection. Both staying home leads to no infection, but also generates zero utility for anyone. The two mixed outcomes, where only one party stays home, also do not lead to infection, and have the advantage that the population that continues to be mobile generates positive utilities.[††] As governments aim to return to higher levels of economic and social activities, such an outcome, with the sick rather than the healthy doing most of the staying at home, will likely become the goal.

Concluding remarks

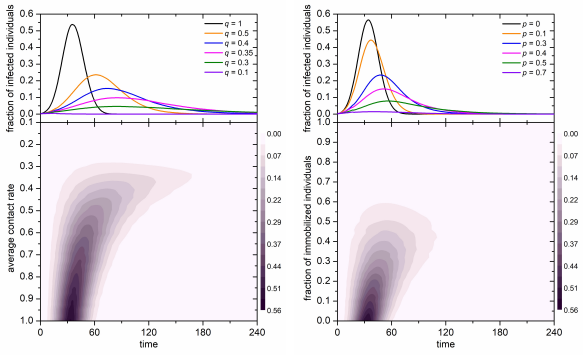

Fig. 2. Left: The color map encodes the fraction of infected individuals in dependence on time and the average contact rate. The upper panel shows characteristic cross-sections of the color map, where it can be observed that the endogenous contact reduction effect is matched no sooner than at 60-70% reduction of the contact rate (average mobility). Right: The color map encodes the fraction of infected individuals in dependence on time and the fraction of immobilized individuals. The upper panel shows characteristic cross-sections of the color map, where it can be observed that the endogenous contact reduction effect is matched no sooner than at 40-50% immobilization. Results were obtained by averaging outcomes over 1.5 million nodes in network configurations that are representative for real social networks. See Appendix C for details.

Here, we have developed a rational-choice framework for differential (health-dependent) levels of social

††Similarly, if the elderly are particularly at risk, either the young or the elderly, or both, should perhaps avoid contacts with one another to avoid infections.

distancing that includes interactive incentives related to risks of infection. A major issue regarding health-dependent analyses of contact rates in general, and to test the kinds of predictions that our model generates in particular, is data availability. To date, very little data is available that records contact rates and health status at the same time. This is hopefully going to change as health-tracking applications are becoming increasingly popular during the ongoing COVID-19 pandemic. Early work indicates that human contacts have reduced markedly in China (53), and that contact rates are crucially important for disease transmission as countries move to lift the lockdowns (16). However, many obstacles remain, especially considering the adherence to recommended behaviours in different societies. We simulated different interpretations of social distancing policies in **Fig.** 2, highlighting what kinds of epidemic curves ought to be expected from either reducing mobility of everyone in the population or from immobilizing a certain fraction.

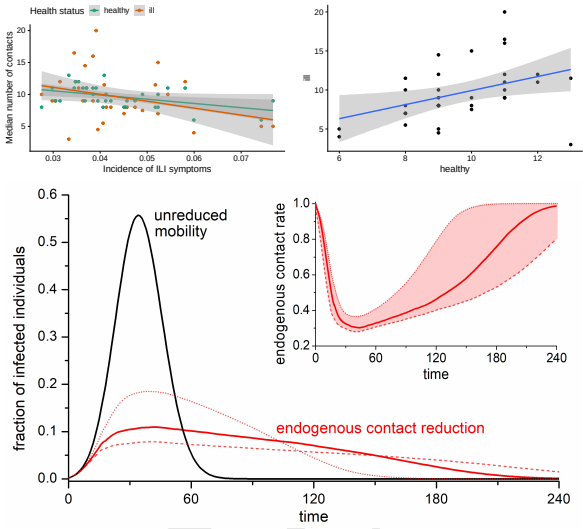

Fig. 3. Top left: Social distancing for sick and healthy. Median number of contacts in any different weeks as a function of incidence of ILI symptoms among Flusurvey participants in that particular week. The lines show linear fits, and shades 95% confidence intervals. Slopes: healthy -70 (95% CI: -120–(-20)), ill -110 (95 %CI: -220, 10); p-value testing null hypothesis of slope 0: healthy 0.01, ill 0.07. Top right: No negative correlation between social distancing rates. Median number of contacts in participants with ILI symptoms as a function of the median number of contacts in participants without ILI symptoms. The lines shows a linear fit, and shades 95% confidence intervals. Slope: 0.9 (95% CI: 0.2-1.6); p-value testing null hypothesis of slope 0: 0.02. Bottom: Comparison of the infected curve, as obtained with unrestrained mobility (black) and endogenous contact reduction based on the Flusurvey data (black). The inset shows how fast the contact rate decreases as the fraction of infected individuals peaks, and then increases comparatively slowly as the incidence of infections decreases. Dashed and dotted lines were obtained with three-fold reductions at 5% and 15%, respectively, as the lower and upper bound on the error from the data (which suggest a three-fold decrease at about 10%).

As a step towards some empirical foundations, we considered Flusurvey data from the United Kingdom (see **Fig.** 3, and Appendix for details), where we found evidence of social distancing amongst healthy individuals as a function of disease incidences in their neighborhoods, as was predicted by our model and by earlier work.[‡‡] The baseline levels of mobility in the UK as recorded per Flusurvey (resulting in medians of circa 12 to 14 contacts per week outside the flu season) are in line with prior estimates from other countries than the UK (39, 54). Indeed, we found that, even in the context of seasonal influenza, some sizeable degree of social distancing took place amongst both sick (mobility reduction of ca. 50-55%) and healthy individuals (mobility reduction of ca. 30-35%), fitting closely phenomena of endogenous social distancing at the population level in other countries (55). Predicted negative correlations between the levels of the two health types were rejected, suggesting presence of behavioral elements beyond individual utility maximization such as social influence, norms, imitation, herding, etc.

The influenza comparison is useful, as seasonal influenza viruses tend to cause less mortal diseases than SARS-COV-2, so any endogenous mobility reductions observed for an influenza according to our model would provide lower bounds on the reductions that we would expect in the current situation (without policy) of a more serious pandemic. In Sweden, for example, where the government decided against the kinds of lockdowns that other European countries implemented, the aggregate population mobility in transit and

[‡‡] Note we pre-registered this type of analysis even though we did not know what kind of data would be available exactly at https://osf.io/zc5b8 and https://osf.io/q3m2p.

workplace decreased by 31% and 11% respectively (as per Google's COVID-19 Community Mobility Report Sweden). This is comparable to the decrease we recorded in the Flusurvey. Our simulations in **Fig.** 3 which use the fit for contact reductions as observed in Flusurvey and extrapolate further reductions in case of incidence levels beyond those observed in Flusurvey indicate that with these kinds of endogenous mobility reductions (as are estimated from real-world behavior in **Fig.** 3) the epidemic curve would have flattened to levels that are comparable in terms of height of the peak and total case numbers as would have been obtained from immobilizing 40-50% of the total population or bringing the average mobility down by 60-70%. These are candidate benchmarks we should be evaluating policy success against.

We are hopeful that future research and applied modeling will make use of game-theoretic modeling to endogenize contact rates in line with a modeling framework we proposed. Further, we encourage future efforts to test our model's hypotheses with more data, as there are potential confounding factors in our data related to the seasonality of contacts because of factors unrelated to disease (especially temperature, but also school holidays etc.), which we cannot account for sufficiently due to data availability. Such analyses are important, as policymakers will likely move to new, perhaps health-status dependent, mobility restrictions and relaxations thereof. Ideally, to evaluate the effectiveness of policies aimed at increasing social distancing there ought to be at least some benchmarking concerning what levels might be expected endogenously during the pandemic, as well as monitoring of individual behaviours in response to changes in government recommendations or restrictions. In particular, the UK COVID-19 lockdown is currently estimated to reduce contacts by 75% (56), which is roughly double the reduction we recorded for healthy individuals for the 2012 and 2013 influenza seasons (see **Fig.** 3), but not substantially above the levels our simulations indicated would justify such policies (see **Fig.** 2). This work suggests scope for future studies in this directions and provides some first measurements.

Governments should factor in endogenous social distancing when weighing the pros and cons of policies as diverse as those ranging from China to Sweden. Epidemic modeling could improve its behavioral micro-foundations more generally.

Materials and Methods

Influenza season contact data. Data for **Fig.** 3 comes from the UK Flusurvey (www.flusurvey.org.uk), an internet platform launched in 2009 to augment existing influenza surveillance (57, 58). The data underlying our analyses is available upon request from S.F.. Its focus is on recording healthcare usage by individuals with influenza-like-illness (ILI) symptoms (59, 60). During an influenza season, participants receive a weekly reminder to report presence or absence of ILI-related symptoms. When reported, followup questions are asked regarding health-care seeking and other behaviors. Flusurvey data has previously been used to estimate incidence trends (61), to identify risk factors (62), to estimate the effectiveness of vaccination (63), and to quantify health-care seeking behavior (64).

During the four influenza seasons 2009–13, social contact data were also collected, some of which is analyzed here. Participants were asked to report conversational and physical contacts by age group in three types of setting (home, work/school and other), as previously used to model H1N1v influenza (65). Here, we use the total of conversational contacts reported as a proxy for overall contacts, and assessed whether the date at which the contacts were submitted were within the start and end dates of an episode of illness with ILI symptoms (one general symptom out of fever, tiredness, weakness and headache, and one respiratory symptom out of sore throat, cough and shortness of breath). The end date of an episode was considered to be a healthy date. We cleaned the data in the following ways. We removed bad symptom dates (end date before start date, dates after the date at which a response was submitted) in 85 out of 8800 symptom reports. We further removed all participants with fewer than three symptom reports (whether reporting healthy or ill), and removed the first submitted survey report of every participant in order to remove any potential bias from participants signing up only because they were researching influenza-related information. Where the end date of an episode was not reported, the date of the report which stated that the illness had ended was taken as the end date of the episode. Incidence was calculated as number of episodes of illness with ILI symptoms starting in any particular week divided by the number participants submitting a report in that week.

Data presented here are based on results from the UK flusurvey (www.flusurvey.org.uk), which was launched in 2009 as a platform for an internet-based cohort to augment existing influenza surveillance (57, 58), most of which

depends on recording healthcare usage by symptomatic individuals (59, 60) and therefore misses individuals with influenza-like-illness (ILI) who do not seek medical attention. During the influenza season, every participants receives a weekly reminder via email, asking to report presence or absence of ILI-related symptoms. If such symptoms are reported, a number of followup questions are asked regarding health-care seeking and other behaviour. See Figure 4 for the key questions of the Flusurvey relevant for this study.

As well as estimating incidence trends (61), flusurvey data have been used to identify risk factors to ILI (62), to estimate the effectiveness of influenza vaccination (63) and to quantify health-care seeking behaviour (64). During the four influenza seasons 2009–13, social contact data were collected in addition to the ILI-related data. Participants were asked to report conversational and physical contacts by age group in three types of setting (home, work/school and other). These data have previously been used to explain the spread of H1N1v influenza (65).

We used the total of conversational contacts reported as measure of overall contact, and assessed whether the date at which the contacts were submitted were within the start end end date of an episode of illness with ILI symptoms (one general symptom out of fever, tiredness, weakness and headache, and one respiratory symptom out of sore throat, cough and shortness of breath). The end date of an episode was considered to be a healthy date.

We cleaned the data in the following ways: We removed bad symptom dates (end date before start date, dates after the date at which a response was submitted) in 85 out of 8800 symptom reports. We further removed all participants with fewer than three symptom reports (whether reporting healthy or ill), and removed the first submitted survey report of every participant in order to remove any potential bias from participants signing up only because they were researching influenza-related information. Where the end date of an episode was not reported, the date of the report which stated that the illness had ended was taken as the end date of the episode.

Incidence was calculated as number of episodes of illness with ILI symptoms starting in any particular week divided by the number participants submitting a report in that week.

Simulation details. We use random geometric graphs in hyperbolic spaces to generate networks that have heterogeneous degree distributions, strong clustering, and short average path lengths, which are all inherent properties of real social networks (66, 67). By increasing the curvature ζ of the hyperbolic space, we move from networks having exponential to networks having scale-free degree distributions, and from longer to shorter average path lengths, and from weaker to stronger clustering. We thus cover the whole family of networks that are representative for real social networks (68).

On top of these networks, we consider the susceptible-exposed-infectious-recovered (SEIR) model (69, 70), as recently declared suitable for describing the spreading of the COVID-19 disease (71). Initially, we select 0.2% of the nodes uniformly at random and designate them as infected (I). The remaining 99.8% of the nodes are designated as susceptible (S). Moreover, every node i is assigned a contact rate q_i, where $q_i = 0$ means the node is not exposed at all and thus has no way of becoming infected, while $q_i = 1$ means the node is fully exposed to potentially become infected by all the other nodes to which it is connected. We note that q_i can also be interpreted as social distancing or mobility, such that $q_i = 0$ means that node i is not traveling to any of the other nodes to which it is connected and is thus fully isolated, while $q_i = 0.5$ means there is only a 50% chance node i will travel to any of the other nodes to which it is connected. We consider the model without social distancing, such that $q_i = 1$ for all nodes, as well as with uniform social distancing, such that we decrease q_i below one for all nodes. We also consider random social distancing, such that a fraction p of nodes is selected at random and assigned $q_i = 0.1$ instead of $q_i = 1$, and with endogenous social distancing, where we fit the Flusurvey data to account for decreasing q_i as the fraction of infected individuals ρ in the population increases. The function we use is $q_i = 3^{(-10\rho)}$, which yields a three-fold decrease in q_i at 10% of infected in the population.

We perform Monte Carlo simulations of this SEIR model (72), which corresponds to a random sequential update, such that during a full Monte Carlo step (MCS) each node gets a chance once on average to become infected. Each full MCS consist of repeating the following elementary step n times. Firstly, select a node i uniformly at random from the whole network. Secondly, (i) If node i is in state S, choose one neighbor j uniformly at random and visit it with probability q_i. If the neighbor is visited and is in state I, node i becomes infected with probability $w = 0.7$. If, however, the neighbor j is in states S or R nothing happens. (ii) If node i is in state I, then verify if at least $t_r = 15$ full MCS have passed since it became infected. If yes, node i becomes recovered (R), and if no, node i remains infected. (iii) If node i is in state R, nothing happens.

Derivations of comparative statics. We first rearrange H-FOC from Equation 2:

$$
\begin{aligned}
& (1\text{-}f \cdot (1\text{-}[(1\text{-}\beta_S^i)^{n\text{-}|H|} \cdot \beta_i + 1\text{-}\beta_i]))u'(\beta_i) \\
= \quad & f \cdot ((1\text{-}\beta_S^i)^{n\text{-}|H|}\text{-}1)u(\beta_i) \\
\iff \quad & (1 + f \cdot (\text{-}1 + [((1\text{-}\beta_S^i)^{n\text{-}|H|}\text{-}1) \cdot \beta_i + 1]))u'(\beta_i) \\
= \quad & f \cdot ((1\text{-}\beta_S^i)^{n\text{-}|H|}\text{-}1)u(\beta_i)
\end{aligned}
\qquad [6]
$$

We are interested in the partial derivative of Equation 7 along d/df, d/dc, $d/d\beta_S$, and $d/d\beta_H$. As the calculations for the former two and the latter two are very similar we only detail them for d/df and $d/d\beta_S$. The other predictions also follow from similar arguments.

Partial derivative of Equation 7 along d/df:

$$
\begin{aligned}
& & & (1+f\cdot(-1+[((1-\beta_S^i)^{n-|H|}-1)\cdot\beta_i+1]))\cdot u''(\beta_i)\cdot\beta_i' \\
& & + \quad & u'(\beta_i)\Big[-1+[((1-\beta_S^i)^{n-|H|}-1)\cdot\beta_i+1]\Big] \\
& & - \quad & u'(\beta_i)f\cdot[(1-\beta_S^i)^{n-|H|}-1]\cdot\beta_i' \\
& & = \quad & -((1-\beta_S^i)^{n-|H|}-1)\cdot(f\cdot u'(\beta_i)\cdot\beta_i'+u(\beta_i)) \\
& \iff & \quad & \beta_i'\cdot\Big[\overbrace{(1+f\cdot(-1+[((1-\beta_S^i)^{n-|H|}-1)\cdot\beta_i+1]))}^{>0}\cdot\overbrace{u''(\beta_i)}^{<0} \\
& & - \quad & \overbrace{u'(\beta_i)\cdot f\cdot[(1-\beta_S^i)^{n-|H|}-1]}^{=(*)}+\overbrace{u'(\beta_i)\cdot f\cdot((1-\beta_S^i)^{n-|H|}-1)}^{=(*)}\Big] \\
& & = \quad & -u'(\beta_i)\Big[-1+[((1-\beta_S^i)^{n-|H|}-1)\cdot\beta_i+1]\Big] \\
& & - \quad & ((1-\beta_S^i)^{n-|H|}-1)\cdot u(\beta_i) \\
& \iff & \quad & \beta_i'\cdot\Big[\overbrace{(1+f\cdot(-1+[((1-\beta_S^i)^{n-|H|}-1)\cdot\beta_i+1]))\cdot u''(\beta_i)}^{<0}\Big] \\
& & = \quad & \overbrace{u'(\beta_i)\Big[-1+[((1-\beta_S^i)^{n-|H|}-1)\cdot\beta_i+1]\Big]}^{>0} \\
& & + \quad & \overbrace{(1-(1-\beta_S^i)^{n-|H|})\cdot u(\beta_i)}^{>0} \\
& & \Rightarrow \quad & \beta_i'<0
\end{aligned}
$$

Partial derivative of Equation 7 along $d/d\beta_S$:

$$
\begin{aligned}
& & & (1+f\cdot(-1+[((1-\beta_S^i)^{n-|H|}-1)\cdot\beta_i+1]))\cdot u''(\beta_i)\cdot\beta_i' \\
& & + \quad & u'(\beta_i)\cdot f\cdot\Big[((1-\beta_S^i)^{n-|H|}-1)\beta_i'-\beta_i(1-\beta_S^i)^{n-|H|-1}\Big] \\
& & = \quad & -f\cdot((1-\beta_S^i)^{n-|H|}-1)\cdot u'(\beta_i)\cdot\beta_i' \\
& & + \quad & f\cdot(1-\beta_S^i)^{n-|H|-1}\cdot u(\beta_i) \\
& \iff & \quad & \beta_i'\cdot\Big[\overbrace{(1+f\cdot(-1+[((1-\beta_S^i)^{n-|H|}-1)\cdot\beta_i+1]))\cdot u''(\beta_i)}^{<0} \\
& & + \quad & \overbrace{u'(\beta_i)\cdot f\cdot((1-\beta_S^i)^{n-|H|}-1)}^{<0} \\
& & + \quad & \overbrace{u'(\beta_i)\cdot f\cdot((1-\beta_S^i)^{n-|H|}-1)}^{<0}\Big] \\
& & = \quad & \overbrace{u'(\beta_i)\cdot f\cdot\beta_i(1-\beta_S^i)^{n-|H|-1}}^{>0} \\
& & + \quad & \overbrace{f\cdot(1-\beta_S^i)^{n-|H|-1}\cdot u(\beta_i)}^{>0} \\
& & \Rightarrow \quad & \beta_i'<0
\end{aligned}
$$

Supporting Information Appendix (SI). The data underlying the analyses of this article is available upon request from S.F..

ACKNOWLEDGMENTS. We are thankful for comments from several colleagues, in particular from Petra Klepac and Bernhard von Stengel. S.F. was funded by a Wellcome Trust Senior Research Fellowship (210758/Z/18/Z). M.G. acknowledges funding from the Slovenian Research Agency (Grant no. P3-0396). We thank the participants

Flu is spread via social contacts. Measuring how we meet each other helps understand and predict flu epidemics. Think about the all people you met yesterday and where you met them.

NOTE: If you are filling this in on behalf of someone else, please answer all the questions as if you are that person

How many people did you have conversational contact with yesterday (talking face to face)?

	0-4 years	5-18 years	19-44 years	45-64 years	65+ years
Home	0	0	0	0	0
Work	0	0	0	0	0
Other	0	0	0	0	0

How many people did you have physical contact with yesterday (skin-to-skin contact, e.g. handshake, kiss)?

	0-4 years	5-18 years	19-44 years	45-64 years	65+ years
Home	0	0	0	0	0
Work	0	0	0	0	0
Other	0	0	0	0	0

How much time did you spend on public transport (e.g. bus, train, underground) yesterday?

- No time at all
- 0-30 minutes
- 30 minutes - 1.5 hours
- 1.5 hours - 4 hours
- Over 4 hours

How long did you spend in an enclosed indoor space (e.g. office, classroom, bar, cinema) with more than 10 other people yesterday? (Not including public transport)

- No time at all
- 0-30 minutes
- 30 minutes - 1.5 hours
- 1.5 hours - 4 hours
- Over 4 hours

What was the furthest distance from home that you travelled yesterday?

- Under 1 mile
- 1-4 miles
- 5-9 miles
- 10-29 miles
- 30-100 miles
- Over 100 miles

Fig. 4. Key questions from the flu survey: the contact survey as seen by flusurvey participants.

of Flusurvey and the Influenzanet consortium who have enabled this study to be performed. Influenzanet were supported by the EU FP7 Epiwork project (grant number 231807) and Flusurvey received additional support from the i-sense (EPSRC IRC in Early Warning Sensing Systems for Infectious Diseases) Exploratory Project. M.U.G.K. acknowledges funding from the Branco Weiss Fellowship, Oxford Martin School and European Horizon 2020 Programme project MOOD. H.H.N. acknowledges an SNF Eccellenza Grant from the Swiss National Science Foundation. M.P. acknowledges funding from the Slovenian Research Agency (Grant nos. J4-9302, J1-9112, and P1-0403).

1. MU Kraemer, et al., The effect of human mobility and control measures on the COVID-19 epidemic in China. *Science* (2020).
2. S Funk, M Salathé, VA Jansen, Modelling the influence of human behaviour on the spread of infectious diseases: a review. *J. Royal Soc. Interface* **7**, 1247–1256 (2010).
3. P Manfredi, A D'Onofrio, *Modeling the interplay between human behavior and the spread of infectious diseases.* (Springer Science & Business Media), (2013).
4. F Verelst, L Willem, P Beutels, Behavioural change models for infectious disease transmission: a systematic review (2010–2015). *J. The Royal Soc. Interface* **13**, 20160820 (2016).
5. CT Bauch, AP Galvani, DJ Earn, Group interest versus self-interest in smallpox vaccination policy. *Proc. Natl. Acad. Sci.* **100**, 10564–10567 (2003).
6. CT Bauch, DJ Earn, Vaccination and the theory of games. *Proc. Natl. Acad. Sci.* **101**, 13391–13394 (2004).
7. AP Galvani, TC Reluga, GB Chapman, Long-standing influenza vaccination policy is in accord with individual self-interest but not with the utilitarian optimum. *Proc. Natl. Acad. Sci.* **104**, 5692–5697 (2007).
8. M van Boven, D Klinkenberg, I Pen, FJ Weissing, H Heesterbeek, Self-interest versus group-interest in antiviral control. *PLoS One* **3** (2008).
9. TC Reluga, An sis epidemiology game with two subpopulations. *J. Biol. Dyn.* **3**, 515–531 (2009).
10. P Poletti, B Caprile, M Ajelli, A Pugliese, S Merler, Spontaneous behavioural changes in response to epidemics. *J. Theor. Biol.* **260**, 31–40 (2009).
11. TC Reluga, Game theory of social distancing in response to an epidemic. *PLoS Comput. Biol.* **6** (2010).
12. D Adam, Special report: The simulations driving the world's response to COVID-19. *Nature* (2020).
13. N Ferguson, et al., Report 9: Impact of non-pharmaceutical interventions (NPIs) to reduce COVID19 mortality and healthcare demand. *Work. Pap.* (2020).
14. S Zhao, CT Bauch, D He, Strategic decision making about travel during disease outbreaks: a game theoretical approach. *J. The Royal Soc. Interface* **15**, 20180515 (2018).
15. S Flaxman, S Mishra, A Gandy, , et al., Estimating the number of infections and the impact of non-pharmaceutical interventions on COVID-19 in 11 European countries. *Imp. Coll. preprint* (2020).
16. L Ferretti, et al., Quantifying SARS-CoV-2 transmission suggests epidemic control with digital contact tracing. *Science* (2020).
17. R Ross, An application of the theory of probabilities to the study of a priori pathometry. Part I. *Proc. Royal Soc. A* **92111184**, 204–230 (1916).
18. R Ross, HP Hudson, An application of the theory of probabilities to the study of a priori pathometry. Part III. *Math. Phys. Character* **93**, 225–240 (1917).
19. R Ross, HP Hudson, An application of the theory of probabilities to the study of a priori pathometry. Part II. *Math. Phys. Character* **93**, 212–225 (1917).
20. WO Kermack, AG McKendrick, Mathematical theory of epidemics. Part II. The problem of endemicity. *Proc. Royal Soc. A* **115**, 55–73 (1927).
21. WO Kermack, AG McKendrick, A contribution to the mathematical theory of epidemics. *Proc. Royal Soc. A* **115**, 700–721 (1927).
22. RM Anderson, R May, *Infectious diseases of humans: dynamics and control.* (Oxford University Press, Oxford, U.K.), (1991).
23. H Heesterbeek, et al., Modeling infectious disease dynamics in the complex landscape of global health. *Science* **347** (2015).
24. M Litvinova, QH Liu, ES Kulikov, M Ajelli, Reactive school closure weakens the network of social interactions and reduces the spread of influenza. *Proc. Natl. Acad. Sci.* (2019).
25. S Cauchemez, et al., Household transmission of 2009 pandemic influenza A (H1N1) virus in the United States. *New Engl. J. Medicine* **361**, 2619–27 (2009).
26. JM Read, WJ Edmunds, S Riley, J Lessler, DA Cummings, Close encounters of the infectious kind: methods to measure social mixing behaviour. *Epidemiol. Infect.* **140**, 2117–2130 (2012).
27. J Wallinga, P Teunis, M Kretzschmar, Using data on social contacts to estimate age-specific transmission parameters for respiratory-spread infectious agents. *Am. J. Epidemiol.* **164**, 936–44 (2006).
28. J Mossong, et al., Social contacts and mixing patterns relevant to the spread of infectious diseases. *PLoS Medicine* **5**, e74 (2008).
29. S Cauchemez, et al., Role of social networks in shaping disease transmission during a community outbreak of 2009 H1N1 pandemic influenza. *Proc. Natl. Acad. Sci.* **108**, 2825–30 (2011).
30. S Cauchemez, F Carrat, C Viboud, AJ Valleron, PY Boëlle, A Bayesian MCMC approach to study transmission of influenza: Application to household longitudinal data. *Stat. Medicine* **23**, 3469–3487 (2004).
31. C Viboud, et al., Synchrony, waves, and spatial hierarchies in the spread of influenza. *Science* **312**, 447–51 (2006).
32. MUG Kraemer, et al., Spread of yellow fever virus outbreak in Angola and the Democratic Republic of the Congo 2015–16: a modelling study. *The Lancet Infect. Dis.* **17**, 330–338 (2017).
33. MC González, Ca Hidalgo, AL Barabási, Understanding individual human mobility patterns. *Nature* **453**, 779–82 (2008).
34. J Candia, et al., Uncovering individual and collective human dynamics from mobile phone records. *J. Phys. A: Math. Theor.* **41**, 224015 (2008).
35. F Simini, MC González, A Maritan, AL Barabási, A universal model for mobility and migration patterns. *Nature* **484**, 96–100 (2012).
36. L Alessandretti, P Sapiezynski, V Sekara, S Lehmann, A Baronchelli, Evidence for a conserved quantity in human mobility. *Nat. Hum. Behav.* **2**, 485 (2018).
37. DL Luh, ZS You, SC Chen, Comparison of the social contact patterns among school-age children in specific seasons, locations, and times. *Epidemics* **14**, 36–44 (2016).
38. KV Kerckhove, N Hens, WJ Edmunds, KTD Eames, The impact of illness on social networks: Implications for transmission and control of influenza. *Am. J. Epidemiol.* **178**, 1655–1662 (2013).
39. F DeStefano, et al., Factors associated with social contacts in four communities during the 2007–2008 influenza season. *Epidemiol. & Infect.* **139**, 1181–1190 (2011).
40. M Kraemer, et al., Progress and challenges in infectious disease cartography. *Trends Parasitol.* **32**, 19–29 (2016).
41. X Lu, L Bengtsson, P Holme, Predictability of population displacement after the 2010 Haiti earthquake. *Proc. Natl. Acad. Sci.* **109**, 11576–11581 (2012).
42. CM Peak, et al., Population mobility reductions associated with travel restrictions during the Ebola epidemic in Sierra Leone: use of mobile phone data. *Int. J. Epidemiol.*, 1–9 (2018).
43. EHY Lam, et al., The feasibility of age-specific travel restrictions during influenza pandemics. *Theor. Biol. Med. Model.* **8**, 1–14 (2011).
44. EP Fenichel, et al., Adaptive human behavior in epidemiological models. *Proc. Natl. Acad. Sci.* **108**, 6306–6311 (2011).
45. D Centola, J Becker, D Brackbill, A Baronchelli, Experimental evidence for tipping points in social convention. *Science* **360**, 1116–1119 (2018).
46. D Centola, A Baronchelli, The spontaneous emergence of conventions: An experimental study of cultural evolution. *Proc. Natl. Acad. Sci.* **112**, 1989–1994 (2015).
47. HP Young, The dynamics of social innovation. *Proc. Natl. Acad. Sci.* **108**, 21285–21291 (2011).
48. K Nyborg, et al., Social norms as solutions. *Science* **354**, 42–43 (2016).
49. H Hu, K Nigmatulina, P Eckhoff, The scaling of contact rates with population density for the infectious disease models. *Math. Biosci.* **244**, 125 – 134 (2013).
50. D McAdams, Nash SIR: An Economic-Epidemiological Model of Strategic Behavior During a Viral Epidemic. *Covid Econ. CEPR (forthcoming)* (2020).
51. F Toxvaerd, Equilibrium Social Distancing. *Covid Econ. CEPR 15* (2020).
52. P Poletti, M Ajelli, S Merler, Risk perception and effectiveness of uncoordinated behavioral responses in an emerging epidemic. *Math. Biosci.* **238**, 80–89 (2012).
53. J Zhang, et al., Age profile of susceptibility, mixing, and social distancing shape the dynamics of the novel coronavirus disease 2019 outbreak in China. *medRxiv* (2020).
54. M Kretzschmar, RT Mikolajczyk, Contact profiles in eight european countries and implications for modelling the spread of airborne infectious diseases. *PloS one* **4** (2009).
55. P Poletti, M Ajelli, S Merler, The effect of risk perception on the 2009 H1N1 pandemic influenza dynamics. *PloS one* **6** (2011).
56. CI Jarvis, et al., Quantifying the impact of physical distance measures on the transmission of covid-19 in the uk. *medRxiv* (2020).
57. I Friesema, et al., Internet-based monitoring of influenza-like illness in the general population: experience of five influenza seasons in The Netherlands. *Vaccine* **27**, 6353–6357 (2009).
58. NL Tilston, KT Eames, D Paolotti, T Ealden, WJ Edmunds, Internet-based surveillance of influenza-like-illness in the UK during the 2009 H1N1 influenza pandemic. *BMC Public Heal.* **10**, 650 (2010).
59. D Fleming, A Elliot, Lessons from 40 years' surveillance of influenza in England and Wales. *Epidemiol. & Infect.* **136**, 866–875 (2008).
60. AJ Elliot, et al., Monitoring the emergence of community transmission of influenza A/H1N1 2009 in England: a cross sectional opportunistic survey of self sampled telephone callers to NHS Direct. *BMJ* **339**, b3403 (2009).
61. E Brooks-Pollock, N Tilston, WJ Edmunds, KT Eames, Using an online survey of healthcare-seeking behaviour to estimate the magnitude and severity of the 2009 H1N1v influenza epidemic in England. *BMC Infect. Dis.* **11**, 68 (2011).
62. AJ Adler, KT Eames, S Funk, WJ Edmunds, Incidence and risk factors for influenza-like-illness in the UK: online surveillance using Flusurvey. *BMC Infect. Dis.* **14**, 232 (2014).
63. K Eames, et al., Rapid assessment of influenza vaccine effectiveness: analysis of an internet-based cohort. *Epidemiol. & Infect.* **140**, 1309–1315 (2012).
64. M Peppa, WJ Edmunds, S Funk, Disease severity determines health-seeking behaviour amongst individuals with influenza-like illness in an internet-based cohort. *BMC Infect. Dis.* **17**, 238 (2017).
65. K Eames, NL Tilston, E Brooks-Pollock, WJ Edmunds, Measured dynamic social contact patterns explain the spread of H1N1v influenza. *PLOS Comput. Biol.* **8**, 1–8 (2012).
66. M Boguná, F Papadopoulos, D Krioukov, Sustaining the internet with hyperbolic mapping. *Nat. Commun.* **1**, 62 (2010).
67. D Krioukov, F Papadopoulos, M Kitsak, A Vahdat, M Boguná, Hyperbolic geometry of complex networks. *Phys. Rev. E* **82**, 036106 (2010).
68. K Zuev, M Boguná, G Bianconi, D Krioukov, Emergence of soft communities from geometric preferential attachment. *Sci. Rep.* **5**, 9421 (2015).

69. R Pastor-Satorras, C Castellano, P Van Mieghem, A Vespignani, Epidemic processes in complex networks. *Rev. Mod. Phys.* **87**, 925 (2015).
70. Z Wang, et al., Statistical physics of vaccination. *Phys. Reports* **664**, 1–113 (2016).
71. K Prem, et al., The effect of control strategies to reduce social mixing on outcomes of the COVID-19 epidemic in Wuhan, China: a modelling study. *Lancet Public Heal.* (2020).
72. MEJ Newman, GT Barkema, *Monte Carlo Methods in Statistical Physics*. (Oxford University Press, Oxford, U.K.), (1999).